Baligh, M. M. (1987). *Géotechnique* **37**, No. 4, 525–527

Undrained deep penetration, I: shear stresses

M. M. BALIGH (1986). *Géotechnique* **36**, No. 4, 471–485

C. I. Teh and G. T. Houlsby, *Oxford University*

The Author has presented an interesting analysis of the undrained deep penetration problem using the strain path method. The simple pile solution has clearly demonstrated the two-dimensional nature of the deep penetration problem which is ignored by the cavity expansion approach. The result revealed some important characteristics of this problem including strain and stress reversals which are not evident in the cavity expansion solution.

The Author derived the stress path in the elastic zone from the closed form solution (Baligh, 1985) for strains. These analytical expressions for strains were based on the simplifying assumption that the streamlines are parallel to the pile axis. Thus, the solution is approximate and applies only in the region where the streamlines are nearly straight. However, for a soil with a low stiffness-to-strength ratio, the elastic–plastic boundary may lie in a region (close to the pile) where the streamlines are significantly curved. Clearly then, derivation of the stress path based on a simplified strain expression would not be appropriate. By taking into consideration the profile of the streamlines, the Writers have obtained the exact analytical expressions for strains around a simple pile.

The geometry of the problem is illustrated in Fig. 1.

STRAIN PATH

The strain ε_{ij} at any point along the streamline is defined as

$$\varepsilon_{ij} = \int \dot{\varepsilon}_{ij}\,\mathrm{d}t + \varepsilon_0 \qquad (1)$$

where $\dot{\varepsilon}_{ij}$ is the strain rate tensor. The in situ strain in the soil, ε_0, can be assumed to be zero without loss of generality. Then

$$\varepsilon_{ij} = \int \dot{\varepsilon}_{ij}\,\mathrm{d}t = \int \dot{\varepsilon}_{ij}\,\frac{\mathrm{d}S}{V} \qquad (2)$$

where dS is the infinitesimal arc length along the streamline and V is the velocity of the soil element. For the simple pile, equation (2) can be transformed into a function of ϕ only. Integrating equation (2) along the streamline yields the following analytical expressions

$$\varepsilon_r = \mathrm{F}_1(\phi) + (1 - \tfrac{3}{2}B^2)\,\mathrm{F}_2(\phi) \qquad (3)$$

$$\varepsilon_z = -\mathrm{F}_1(\phi) - \tfrac{1}{2}(1 - 3B^2)\,\mathrm{F}_2(\phi) \qquad (4)$$

$$\varepsilon_\theta = -\tfrac{1}{2}\,\mathrm{F}_2(\phi) \qquad (5)$$

$$\varepsilon_{rz} = -\frac{3}{2}\left\{(2B^2 - 1)\left(\frac{\pi - \phi}{2}\right) + B\sin\phi - \frac{\sin(2\phi)}{4} - 2B(B^2 - 1)^{0\cdot 5} \times \tan^{-1}\left[\left(\frac{B+1}{B-1}\right)^{0\cdot 5}\cot\left(\frac{\phi}{2}\right)\right]\right\} \qquad (6)$$

where

$$\mathrm{F}_1(\phi) = 3(1 + \cos\phi)\left[\left(\frac{r_0}{R}\right)^2 + \frac{3}{4} - \frac{\cos\phi}{4}\right] \qquad (7)$$

$$\mathrm{F}_2(\phi) = \ln\left[1 + \frac{1}{2}\left(\frac{r_0}{R}\right)^2(1 + \cos\phi)\right] \qquad (8)$$

$$B = 2\left(\frac{r_0}{R}\right)^2 + 1 \qquad (9)$$

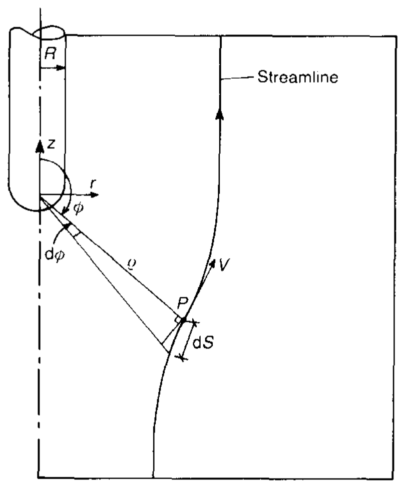

Fig. 1. Simple pile problem: geometry of the strain path solution

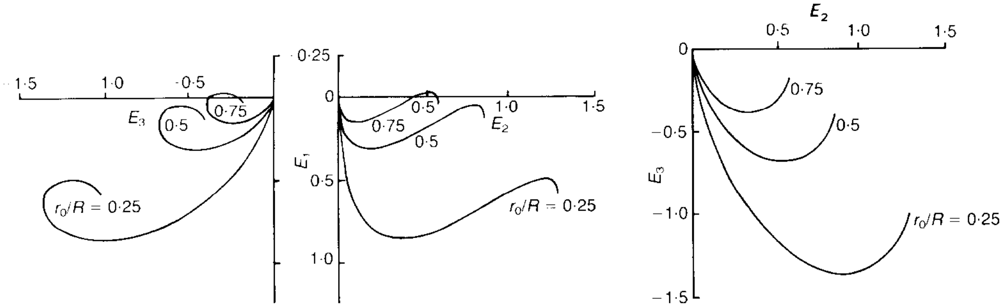

Fig. 2. Strain paths in the near field of a simple pile

R is the limit radius of the simple pile and r_0 is the initial radial distance of the streamline. Equations (3)–(6) are applicable in both the far field and the near field of the pile. When the initial location of the streamline is very large ($r_0 \gg 1$) but not infinite, the leading order terms of these strain components can be shown to be identical with the approximate far field solutions given by the Author.

When equations (3)–(6) are plotted using the strain deviators E_1, E_2 and E_3 as defined by the Author, the strain paths in the far field are virtually identical with those given by the Author. However, as r_0/R decreases (close to the pile shaft), the projections of the strain path on the E_i plane (Fig. 2) take on a progressively skewed appearance. The results obtained numerically by Baligh (1985) show the same trend. The following points are evident from Fig. 2

(*a*) in both the near field and the far field, E_2 increases monotonically, but E_1 and E_3 exhibit significant strain reversals
(*b*) in the near field, as $z \to \infty$ ($\phi \to 0$), both E_1 and E_3 are no longer zero (as in the far field) but have finite residual values.

STRESS PATH

Given the strain path, the stress path (including the initial elastic response) can be derived by adopting a suitable constitutive relationship for the soil. For comparison, the Writers adopted the same bilinear Prandtl–Reuss model with the Von Mises yield criterion as used by the Author. The strain increment between any two points on the streamline can be determined exactly using equation (3). The stress–strain relationship has been accurately integrated using small strain increments and a closed form solution due to Booker (1984). This solution relates the stress increment due to a corresponding strain increment and is applicable only to the zero rotation rate case, which applies for the assumed inviscid flow strain rate solution.

For a soil with $G/k = 100$, the stress paths thus obtained are plotted in Figs 3 and 4. Fig. 3 shows the stress paths for soil elements initially located at radial distances R, $5R$, $10R$ and $15R$ from the pile axis. These results are comparable with those given by the Author. In the inner plastic zone, however, there is a significant difference between the Writers' results and the Author's limit solution. Fig. 4 shows the stress path of a soil element

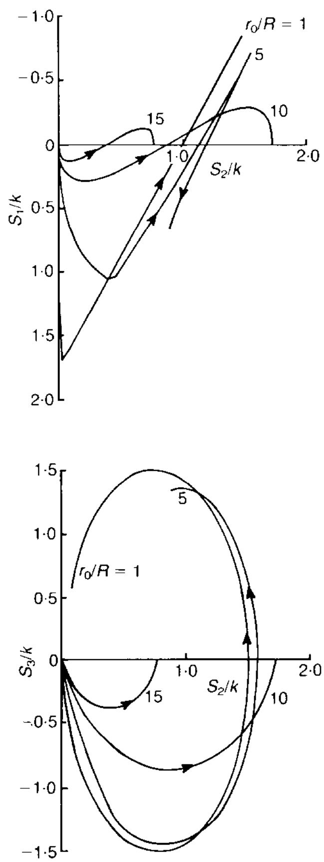

Fig. 3. Stress paths of soil elements initially at different radial distances r_0/R

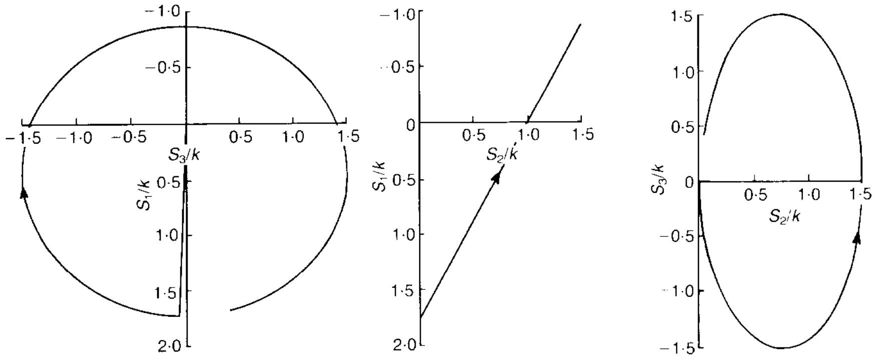

Fig. 4. Stress path in the inner plastic zone: $r_0/R = 0{\cdot}01$

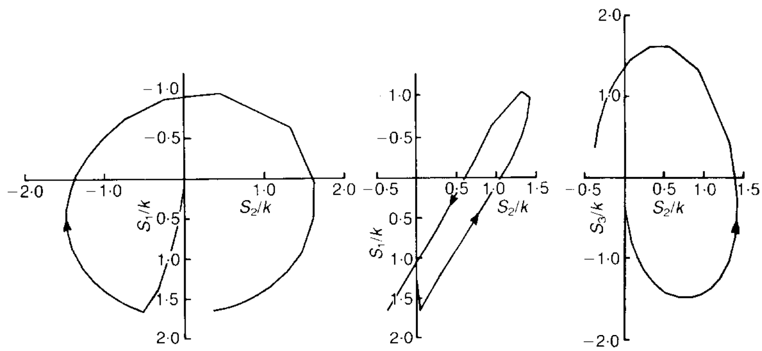

Fig. 5. Stress path in the near field of a 60° cone penetrometer: $r_0/R = 1{\cdot}0$

initially located at $r_0 = 0{\cdot}01R$. Far behind the pile tip (as $z \to \infty$, $\phi \to 0$), the stress deviator S_3 has a finite value. This should be compared with the Author's solution which indicates that $S_3 = 0$ on the shaft.

The present solution shows that the shear stress in the immediate vicinity of the pile shaft is not zero even though the strain field is based on an inviscid flow solution. This stress state therefore does not correspond to a simple pile with a smooth shaft as the Author's result would suggest. One possible explanation for the difference in S_3 might be the inclusion of the initial elastic response in the stress calculation. The Writers recognize that the strain path method yields only an approximate solution because the equilibrium equations are not fully satisfied. Nevertheless, it is essential to resolve the discrepancy regarding the value of S_3 close to the shaft before the result can be used to interpret pile installation and deep penetration problems in a meaningful way.

The Writers have also analysed the problem of a cone penetrometer with a 60° tip using a numerical approach. The stress paths in the far field of the penetrometer are virtually identical with those of the simple pile. This indicates that the simple pile solution can be used to estimate the stress state in the far field of a cone penetrometer. However, there are significant differences in the near field solutions. Fig. 5 shows the stress path of a soil element initially located at $r_0/R = 1{\cdot}0$ from the axis of the penetrometer. A comparison of Figs 3 and 5 shows that near field stress paths are significantly affected by the shape of the penetrometer. It is therefore reasonable to conclude that in a rational analysis of the penetrometer the actual geometry of the cone (more specifically, the cone angle) must be taken into consideration.

REFERENCES

Baligh, M. M. (1985). Strain path method. *J. Geotech. Engng Div. Am. Soc. Civ. Engrs* **111**, GT9, 1109–1135.

Booker, J. R. (1984). Private communication.